AD-A155628

AD E440281

TECHNICAL REPORT ARLCB-TR-85011

STRESS CONCENTRATION IN THE ELASTOPLASTIC STATE AND RESIDUAL STRESS AFTER UNLOADING

Y. F. CHENG

MARCH 1985

US ARMY ARMAMENT RESEARCH AND DEVELOPMENT CENTER
LARGE CALIBER WEAPON SYSTEMS LABORATORY
BENÉT WEAPONS LABORATORY
WATERVLIET N.Y. 12189

APPROVED FOR PUBLIC RELEASE; DISTRIBUTION UNLIMITED

DISCLAIMER

The findings in this report are not to be construed as an official Department of the Army position unless so designated by other authorized documents.

The use of trade name(s) and/or manufacture(s) does not constitute an official indorsement or approval.

DISPOSITION

Destroy this report when it is no longer needed. Do not return it to the originator.

SECURITY CLASSIFICATION OF THIS PAGE (When Data Entered)

REPORT DOCUMENTATION PAGE

READ INSTRUCTIONS BEFORE COMPLETING FORM

1. REPORT NUMBER: ARLCB-TR-85011	2. GOVT ACCESSION NO.
3. RECIPIENT'S CATALOG NUMBER	
4. TITLE (and Subtitle): STRESS CONCENTRATION IN THE ELASTOPLASTIC STATE AND RESIDUAL STRESS AFTER UNLOADING	5. TYPE OF REPORT & PERIOD COVERED: Final
	6. PERFORMING ORG. REPORT NUMBER
7. AUTHOR(s): Y. F. Cheng	8. CONTRACT OR GRANT NUMBER(s)
9. PERFORMING ORGANIZATION NAME AND ADDRESS: US Army Armament Research & Development Center, Benet Weapons Laboratory, SMCAR-LCB-TL, Watervliet, NY 12189-5000	10. PROGRAM ELEMENT, PROJECT, TASK AREA & WORK UNIT NUMBERS: AMCMS No. 6111.02.H600.011, PRON No. 1A425M541A1A
11. CONTROLLING OFFICE NAME AND ADDRESS: US Army Armament Research & Development Center, Large Caliber Weapon Systems Laboratory, Dover, NJ 07801-5001	12. REPORT DATE: March 1985
	13. NUMBER OF PAGES: 32
14. MONITORING AGENCY NAME & ADDRESS (if different from Controlling Office)	15. SECURITY CLASS. (of this report): UNCLASSIFIED
	15a. DECLASSIFICATION/DOWNGRADING SCHEDULE

16. DISTRIBUTION STATEMENT (of this Report)

Approved for public release; distribution unlimited.

17. DISTRIBUTION STATEMENT (of the abstract entered in Block 20, if different from Report)

18. SUPPLEMENTARY NOTES

Presented at 1984 Army Symposium on Solid Mechanics, Newport, Rhode Island, 1-3 October 1984.

19. KEY WORDS (Continue on reverse side if necessary and identify by block number)

Photoelasticity	Elastoplastic State
Photoplasticity	Stress Concentration
Photoelastic Coating	Residual Stress

20. ABSTRACT (Continue on reverse side if necessary and identify by block number)

Photoplasticity and photoelastic coating techniques have been successfully employed to study stress concentration in the elastoplastic state and residual stress after unloading. Principles are described herein, and examples of the application of both methods are given. The results show that stress concentration in the elastoplastic state is lower than that in the elastic state and decreases continuously as yielding progresses. A good agreement exists between results from both methods.

DD FORM 1 JAN 73 1473 EDITION OF 1 NOV 65 IS OBSOLETE

UNCLASSIFIED

SECURITY CLASSIFICATION OF THIS PAGE (When Data Entered)

TABLE OF CONTENTS

TABLES

LIST OF ILLUSTRATIONS

ACKNOWLEDGEMENT

Charles Cobb's participation in the experimental phase of this investigation is hereby acknowledged.

INTRODUCTION

It is well-known that in certain structural members an initial tensile overload produces a beneficial compressive residual stress upon unloading. This fact has been utilized extensively in armament designs such as breech rings to reduce their operating stresses and to improve their fatigue lives. It is also known that stress concentrations in the elastoplastic state are different from those in the elastic state (ref 1). Thus, elastic stress concentration factors cannot be used to calculate the maximum stress at overload. This report describes two experimental methods; namely, photoplasticity and photoelastic coatings, for determining stress concentration factors in the elastic and elastoplastic states. Basic principles are stated herein, along with examples of the application of both methods. Maximum free boundary stress at overload, elastic-plastic boundary, and residual stress after unloading are found. The results show that stress concentration in the elastoplastic state is lower than that in the elastic state and decreases continuously as yielding progresses.

PHOTOPLASTICITY

Experimental Method

Photoelastic stress analysis is based on the linear stress-optic law (refs 2,3). The discovery of the non-linear stress-optic law extends the

---

[1]Thomson, R. A. and Frocht, M. M., "Further Work on Plane Elastoplastic Stress Distributions," Proceedings of the International Symposium on Photoelasticity, IIT, Chicago, 1961, pp. 185-193.
[2]Coker, E. G. and Filon, L. H. G., A Treatise on Photoelasticity, Second Edition, Cambridge University Press, 1957.
[3]Frocht, M. M., Photoelasticity, John Wiley and Sons, 1958.

photoelastic method to the plastic state (ref 4). Specifically, at any point in a model, the isochromatic fringe is related to the secondary principal stress difference ($\sigma_1' - \sigma_2'$), and the isoclinic parameter gives the directions of the secondary principal stresses σ_1' and σ_2'. In two-dimensional cases, the secondary principal stresses become principal stresses σ_1 and σ_2.

In this report, we are interested only in the boundary stress and maximum shear in two-dimensional models. No attempts were made to determine the individual stress distribution, although techniques are readily available. On the free boundary, one of the principal stresses is identically zero, and the remaining principal stress tangent to the boundary is given by the boundary fringe order. It is known that the maximum shear, τ_{max}, equals one-half of the principal stress difference; i.e., $\tau_{max} = (\sigma_1 - \sigma_2)/2$. For a material obeying the yield condition of maximum shear, the elastic-plastic boundary is defined by the fringe having a maximum shear of $\sigma_y/2$, where σ_y is the yielding stress.

Model Material

Polycarbonate resin (ester of carbonic acid and bisphenol A) was first suggested by Ito (ref 5) in 1962 for use as model material. It is ductile and has good transparency in both elastic and plastic states. Gurtman et al (ref 6) conducted uniaxial tension tests on flat specimens of polycarbonate in 1965

---

[4] Frocht, M. M. and Cheng, Y. F., "An Experimental Study of the Laws of Double Refraction in the Plastic State in Cellulose Nitrate - Foundations for Three-Dimensional Photoplasticity," Proceedings of the International Symposium on Photoelasticity, IIT, Chicago, 1961, pp. 195-216.

[5] Ito, K., "New Model Materials for Photoelasticity and Photoplasticity," Experimental Mechanics, 2(12), December 1962, pp. 373-376.

[6] Gurtman, G. A., Jenkins, W. C., and Tung, T. K., "Characterization of a Birefringent Material for Use in Photoelastoplasticity," Douglas Report SM 7796, January 1965.

and reported a Poisson's ratio of 0.38 in the elastic state and a limiting value of 0.5 in the plastic state. They also found that polycarbonate creeps optically and mechanically (birefringence and strain) at a stress of above 4000 psi.

The polycarbonate resin used in this work was supplied by the General Electric Company under the trade name LEXAN. It had a thickness of 0.12 inch. Calibration tests were made at a temperature of 73° ± 3°F and a relative humidity of 10% ± 5%. Strain was calculated from deformation readings obtained through a travelling telemicroscope. Birefringence was determined by means of Senarmont's principal of compensation with a collimated monochromatic light of 5461 Å. The results show that this material creeps both optically and mechanically at a stress of above 4000 psi, confirming Gurtman's work, and that both creeps stabilize after 240 minutes. Figures 1 and 2 show the stress-fringe and stress-strain curves. The polycarbonate has an elastic material fringe value of 36 psi per inch, a Young's modulus E of 3.25×10^5 psi, a proportional limit stress of 6.2×10^3 psi, and a secant yield strength, σ_{sec}, defined by the point of intersection of secant modulus ($E_{sec} = 0.7E$) and the stress-strain curve of 8.7×10^3 psi. The non-dimensional stress-strain curve given by the Ramberg-Osgood equation (ref 7) for this material has the following form:

$$E\epsilon/\sigma_{sec} = (\sigma/\sigma_{sec}) + (3/7)(\sigma/\sigma_{sec})^{11.5} \tag{1}$$

---

[7]Ramberg, W. and Osgood, W. R., "Description of Stress-Strain Curves of Three Parameters," NACA TN 902, 1943.

where ε denotes strain, and σ stress. During calibration, Luder's lines were observed, Figure 3, indicating that polycarbonate follows the yield condition of maximum shear.

Experiments and Results

1. Experiments on C-Shaped and Compact Tensile Specimens. The purposes of this series of experiments were to determine stress concentration factors in elastic and plastic states, and residual stresses after unloading. Three models each of the C-shaped and compact tensile specimens, Figures 4 and 5, were made. In order to minimize any effect of material nonhomogeneity, they were cut closely to the calibration specimens with their lines of loading parallel to each other. One model was tested in the elastic state. The other two models were tested in the elastoplastic state. Each elastoplastic test requires a new model. The load was applied through pins.

Photographs of isochromatic fringe pattern were taken for each load at 240 minutes after loading. The fringe and maximum shear distributions across the narrowest section were determined, Figures 6 and 7.

It was mentioned previously that for a material obeying the yield criterion of maximum shear, such as LEXAN, the elastic-plastic boundary is defined by the fringe having a maximum shear of $\sigma_y/2$. In this work, we chose the proportional limit stress of 6.2×10^3 psi as σ_y. Hence, the elastic-plastic boundary was given by the fringe having a maximum shear of 3.1×10^3 psi. The depth of the plastic region on the narrowest section AB, Figures 4 and 5, and its extended angle along the notch were found at two levels of load and are shown in Table I.

TABLE I. SIZE OF PLASTIC REGION

Specimen	Load, Pound	Plastic Region	
		Depth, l/AB	Extended Angle, Degrees
C-shaped	15.2	0.02	50
C-shaped	18.7	0.04	65
Compact	56	0.006	70
Compact	64	0.01	90

Boundary fringe order and stress σ were determined for end points A and B. Stress concentration factor K was defined as the ratio of σ/σ_{nom}, where

$$\sigma_{nom,A} = (P/td)(1+6D/d) \quad (2)$$

and

$$\sigma_{nom,B} = (P/td)(1-6D/d) \quad (3)$$

Subscripts refer to points A and B, respectively. These values are shown in Figure 8 and are listed in Tables II and III.

The results show that as long as the material is in the elastic state, stress varies linearly with the load. Stress concentration factor K is a constant and the K-σ_{nom} curve is straight and horizontal. When load is increased such that local yielding sets in, the linear stress-load relation breaks down and the stress concentration factor decreases continuously as yielding progresses. The stress at point B in the C-shaped specimen is less than the nominal value. Hence, at this point the stress concentration factor is less than one. At 18.7 pounds of load, point B was still in the elastic state, although the plastic region had already progressed to a depth of 0.04 AB from point A. Assuming that the material property in compression is the same as in tension, point B would yield at a load of approximately 6200/(325 x

0.83) = 23 pounds.*

For the purpose of calculating residual stress, the usual assumption that unloading is inherently an elastic process was made. For example, an unloading from 18.7 pounds of load would reduce a stress of (1.53)(352)(18.7) = 10.1×10^3 psi* at point A in the C-shaped specimen. Superposition of this value with 7.85×10^3 psi from elastoplastic load of 18.7 pounds gives a residual stress of 2.22×10^3 psi compression, as shown in Table II.

The percentage of overloading is defined as $[(P/P_p) -1] \times 100\%$ where P_p denotes the proportional limit load, the load that produces the proportional limit stress. The proportional limit load has a value of 11.5 and 41.6 pounds for C-shaped and compact tensile specimens, respectively.

The residual stress and percentage of overloading were calculated for both specimens and are listed in Tables II and III.

2. Experiment on Breech Ring Section. It is known that most breech ring failures are caused by the presence of high tensile stress at the lower fillet. It is also known that by introducing residual compressive stress at the lower fillet, ring failure can be delayed. The purpose of this experiment was to determine the residual stress at the lower fillet in an overloaded breech ring after unloading.

A model of the meridian section of a breech ring was made, Figure 9. It was cut closely to the calibration specimens with their lines of loading parallel to each other. The block was made of aluminum. The top of the ring

---

*In C-shaped specimens, real dimensions give $\sigma_{nom,A} = 352$ P and $\sigma_{nom,B} = 325$ P, respectively.

TABLE II. STRESS CONCENTRATION FACTOR, PERCENTAGE OF OVERLOADING, AND RESIDUAL STRESS IN POLYCARBONATE C-SHAPED SPECIMENS

	Nominal Stress		Boundary Stress		Stress Concentration Factor			
Load (pounds)	σ_{An} (psi)	σ_{Bn} (psi)	σ_A (psi)	σ_B (psi)	K_A	K_B	Percentage of Overloading	Residual Stress (psi)
3.84	1350	-1250	2040	-1050	1.51	0.84		
5.15	1810	-1670	2850	-1410	1.57	0.84		
6.45	2270	-2100	3450	-1710	1.52	0.81		
					Av: 1.53			
15.2	5350	-4940	7000	-4200	1.31	0.85	32	-1190
18.7	6580	-6080	7850	-5000	1.19	0.82	63	-2220
						Av: 0.83		

TABLE III. STRESS CONCENTRATION FACTOR, PERCENTAGE OF OVERLOADING, AND RESIDUAL STRESS IN POLYCARBONATE COMPACT TENSILE SPECIMENS

Load (pounds)	Nominal Stress σ_{An} (psi)	Boundary Stress σA (psi)	Stress Concentration Factor K	Percentage of Overloading	Residual Stress (psi)
8	550	1190	2.16		
12	820	1790	2.18		
16	1090	2380	2.18		
20	1370	2980	2.18		
			Av: 2.18		
56	3830	7500	1.96	35	-840
64	4370	8200	1.88	54	-1330

was fixed. The load was applied through a pin at the top of the block. Guide plates were used to prevent buckling.

Maximum fringe order at the lower fillet was closely watched during loading. The loads corresponding to the first four integral fringes were recorded, Table IV. It was found that in the elastic state a load of 27 pounds was necessary to raise one order of fringe, or 300 psi, at the fillet. After the elastic stress was determined, the load was increased to the elasto-plastic state of 1144 pounds and held for 240 minutes. Maximum fringe order at the fillet was measured intermittently. At 240 minutes it had an order of 43 indicating a plastic stress of 9.3×10^3 psi. A complete unloading would produce a stress reduction of $(1144)(300/27) = 12.7 \times 10^3$ psi giving a residual stress of 3.4×10^3 psi compression.

TABLE IV. LOAD AND FRINGE ORDER AT LOWER FILLET OF A POLYCARBONATE BREECH RING SECTION

Fringe Order	Load, Pound	Remarks
1	23	Elastic
2	51	
3	78	
4	104	
43	1144	Elastoplastic

Transition to Prototype

Solutions of problems in stress distribution, whether elastic or plastic, must satisfy three conditions: equilibrium, compatibility, and boundary

values. The elastic stresses, except those in the immediate vicinity of contact, are proportional directly to the loads and inversely to the square of the scale ratio. The transition of data from model to prototype can be made through the following equation:

$$\sigma_p/\sigma_m = (P_p/P_m)(L_m/L_p)^2 \tag{4}$$

where L is a characteristic length, and subscripts m and p refer to model and prototype, respectively.

The transition of plastic stress from model to prototype requires at least three more conditions: the same shape of non-dimensional stress-strain curves of both materials, the same law of yielding, and the same Poisson's ratio in the plastic state. Elastoplastic data from the polycarbonate model are transferable to prototype material having a Poisson's ratio of 0.5 in the plastic state and obeying the maximum shear yield criterion. By adjusting the temperature and relative humidity of the laboratory, the shape of non-dimensional stress-strain curve of polycarbonate can be altered to closely resemble that of prototype.

PHOTOELASTIC COATING

Experimental Method

The photoelastic coating technique was initially introduced by Mesnager (ref 8) in 1930. The method is based on the bonding of a thin layer of photoelastic material to the surface of the specimen. When load is applied to the

---

[8]Mesnager, M., "Sur la Determination Optique des Tensions Interieures dan les Solides a Trois Dimensions," Compt. Rend. l'Acad. Sci., Vol. 190, 1930, pp. 1249-1250.

specimen, strains are transmitted to the coating which then becomes birefringent. Polarized light is reflected from the surface of the specimen at normal incidence, and fringe patterns are obtained as in the photoelastic method.

Neglecting thickness effect of the reflective layer, the fringe order N is related to the principal strain difference $(\varepsilon_1-\varepsilon_2)$ on the surface of the specimen as

$$N = 2c'_t(\varepsilon_1-\varepsilon_2) \tag{5}$$

where c' denotes the strain-fringe constant, and t thickness of the coating.

In this report, we are interested only in the boundary stress in two-dimensional models, although techniques for separating individual strains and stresses are readily available.

In the elastic state, stress-strain relation has the following form:

$$\varepsilon_1 - \varepsilon_2 = (1+\mu)(\sigma_1-\sigma_2)/E \tag{6}$$

where μ denotes Poisson's ratio. Combining Eqs. (5) and (6), we have

$$\sigma_1 - \sigma_2 = (N/2c'_t)[E/(1+\mu)] \tag{7}$$

On the free boundary one of the principal stresses is identically zero and the remaining principal stress tangent to the boundary can readily be found.

In the plastic state, in addition to Eq. (5), we have

$$\varepsilon_1 + \varepsilon_2 + \varepsilon_3 = 0 \tag{8}$$

where subscript 3 refers to the third principal component acting in the direction perpendicular to the surface. On the free boundary of a plane stress problem we have

$$\sigma_2 = \sigma_3 = 0 \tag{9}$$

and

$$\varepsilon_2 = \varepsilon_3 = -\varepsilon_1/2 \tag{10}$$

The principal strain ε_1 tangent to the free boundary becomes

$$\varepsilon_1 = N/3c't \tag{11}$$

and the corresponding principal stress σ_1 can be found from the uniaxial stress-strain relation of the material.

Model and Coating Materials

Flat ground steel plate of 0.12-inch thickness with a chemical content of 0.85-0.95 C, 1.00-1.25 Mn, 0.20-0.40 Si, 0.40-0.60 Cr, 0.40-0.60 W, and 0.10-0.20 V was used as the model material. It was supplied by Simons Saw and Steel, Fitchburg, MA. Type PS-1 photoelastic sheet of 0.04-inch thickness was used as the coating material. It was supplied by Measurement Group, Raleigh, NC.

Tensile calibration specimens of steel were prepared with electric resistance strain gages (EA-13-015DJ-120, Micromeasurement), which were bonded at the specimen midsections, one gage on each side. Coating was applied on the surface of the specimens. Figure 10 shows the stress-strain curve obtained from strain gage readings. The steel has a Young's modulus E of 30 x 10^6 psi, a proportional limit stress of 51 x 10^3 psi, and a secant yield strength σ_{sec} of 60 x 10^3 psi. Poisson's ratio was taken to be 0.3 in the elastic state. During calibration the coating material registered one fringe per 1890 x 10^{-6} in./in. of axial strain ε_1 or a principal strain difference of

$$\varepsilon_1 - \varepsilon_2 = 1.3\ \varepsilon_1 = 2460 \times 10^{-6} \text{ in./in.} \tag{12}$$

Monochromatic light of 5461 Å was used.

Experiment and Result

Due to the limited availability of the material, a 55/65 scale, two-dimensional model of the meridian section of a breech ring and block was made with its line of loading parallel to those of the calibration specimens. Photoelastic coating was bonded to both surfaces of the lower part of the ring. The boundary of the coating was carefully machined so as to coincide with the fillet. The model was mounted in the Testing Machine (Baldwin-Tate-Emery) and the loads were applied through pins at the top of the block and ring.

It was found that in the elastic state, 2100 pounds of load was required to produce one-half of a fringe, or a principal strain difference ($\varepsilon_1-\varepsilon_2$) of 1230×10^{-6} in./in. at the fillet. On the fillet boundary, $\sigma_2 = 0$, and the maximum fillet stress from Eq. (6)

$$\sigma_1 = E(\varepsilon_1-\varepsilon_2)/(1+\mu) = (30)(1230)/1.3 = 28.4 \times 10^3 \text{ psi} \tag{13}$$

The average stress σ_{av} at the cross-section has a value of

$$\sigma_{av} = 2100/[(0.12)(5.75)(55/65)] = 3.6 \times 10^3 \text{ psi} \tag{14}$$

The stress concentration factor K, defined as the ratio of maximum fillet stress to average stress is

$$K = \sigma_1/\sigma_{av} = 7.88 \tag{15}$$

After the elastic solution was obtained, the model was loaded into the elastoplastic state. The loads corresponding to each increasing integral fringe order were recorded. Principal strain difference ($\varepsilon_1-\varepsilon_2$), maximum principal strain ε_1 and stress σ_1, average stress σ_{av}, stress concentration factor K, and residual stress after unloading were calculated and are listed in Table V.

TABLE V. LOAD, MAXIMUM STRESS, STRESS CONCENTRATION FACTOR, AND RESIDUAL STRESS AT THE LOWER FILLET OF A STEEL BREECH RING SECTION

Load P Pounds	Fringe Order N	Principal Strain Difference $(\varepsilon_1-\varepsilon_2)_s$ in./in.	Maximum Principal Strain $(\varepsilon_1)_s$ in./in.	Maximum Principal Stress $(\sigma_1)_s$ psi	Average Stress σ_{av} psi	Stress Concentration Factor $K = (\sigma_1)_s/\sigma_{av}$	Percentage of Overloading (P-3770)/3770	Residual Stress psi
2100	0.5	1230×10^{-6}	950×10^{-6}	28.4×10^{3}	3.60×10^{3}	7.88	-	-
4100	1	2460×10^{-6}	1870×10^{-6}	54.9×10^{3}	7.02×10^{3}	7.63	9	-0.5×10^{3}
6000	2	4920×10^{-6}	3510×10^{-6}	61.2×10^{3}	10.3×10^{3}	5.96	59	-19.9×10^{3}
7000	3	7380×10^{-6}	5150×10^{-6}	63.1×10^{3}	12.0×10^{3}	5.26	86	-31.6×10^{3}
7600	4	9840×10^{-6}	6790×10^{-6}	64.7×10^{3}	13.0×10^{3}	4.97	102	-38.1×10^{3}
8000	5	12300×10^{-6}	8440×10^{-6}	66.3×10^{3}	13.7×10^{3}	4.84	112	-41.9×10^{3}

Table V and Figure 11 show that as long as the model is in the elastic state, stress concentration factor is constant. When load is increased such that local yielding sets in, stress concentration factor decreases continuously as yielding progresses. These results are consistent with those obtained from photoplasticity experiments.

COMPARISON BETWEEN RESULTS FROM PHOTOELASTOPLASTICITY AND PHOTOELASTIC COATING

Table VI shows a comparison between results obtained from steel and polycarbonate models of breech ring.

TABLE VI. COMPARISON BETWEEN STEEL AND POLYCARBONATE MODELS

		Steel	Polycarbonate
Elastic Static	Load	2100 pounds	27 pounds
	Maximum Fillet Stress	28.4×10^3 psi	300 psi
	Average Stress	3.6×10^3 psi	300 psi
	Stress Concentration Factor	7.88	7.67
Elastoplastic Static	Load	7600 pounds	1144 pounds
	Maximum Fillet Stress	64.7×10^3 psi	9.3×10^3 psi
	Percentage of Overloading	102	105
	Average Stress	13.0×10^3 psi	1.66×10^3 psi
	Stress Concentration Factor	4.97	5.61

In the elastic state, the steel model has a stress concentration factor of 7.88 in comparison with 7.67 from a polycarbonate model. Also, the steel model shows a maximum fillet stress of 28.4×10^3 psi under a load of 2100 pounds in comparison with 27.6×10^3 psi obtained by means of transition, Eq. (4), and data from the polycarbonate model. A good agreement is established.

As mentioned earlier, the transition of data in the elastoplastic state requires at least three additional conditions: same Poisson's ratio, same law of yielding, and same shape of non-dimensional stress-strain curve. A comparison between Figures 2 and 10 clearly shows the violation of the last condition. Specifically, steel and polycarbonate do not have the same shape of non-dimensional stress-strain curves at room temperature, although it is possible to match them closely by adjusting the temperature and relative humidity of the laboratory. Nevertheless, the steel model at 102 percent overloading shows a stress concentration factor of 4.97 in comparison with 5.61 from a 105 percent overloading polycarbonate model. The difference is reasonable.

CONCLUSIONS

Principles of photoplasticity and photoelastic coating have been described. Examples of the application of both methods to a C-shaped notched specimen, a compact tensile notched specimen, and a breech ring section in the elastoplastic state have been given. Maximum free boundary stress, stress concentration in the elastic and plastic state, elastic-plastic boundary, and residual stress after unloading have been determined.

In photoplastic analysis, data in the elastic state are transferable from model to prototype with usual consideration of load and scale ratios. In the plastic state, the transition of data requires at least the satisfaction of three additional conditions on material property: Poisson's ratio, yield criterion, and stress-strain relation. The coating method gives data for models of prototype material. The transition of data requires only the consideration of load and scale ratios.

Stress concentration is constant in the elastic state and decreases continuously as yielding progresses. Therefore, it is advisable to determine stress concentration factor at each load in the elastoplastic state.

Results from photoplasticity and photoelastic coating for a breech ring section have been compared. A reasonable agreement has been reached. The reliability and ease of photoplastic analysis and photoelastic coating technique in the elastoplastic state have been demonstrated.

REFERENCES

1. Thomson, R. A. and Frocht, M. M., "Further Work on Plane Elastoplastic Stress Distributions," Proceedings of the International Symposium on Photoelasticity, IIT, Chicago, 1961, pp. 185-193.

2. Coker, E. G. and Filon, L. H. G., A Treatise on Photoelasticity, Second Edition, Cambridge University Press, 1957.

3. Frocht, M. M., Photoelasticity, John Wiley and Sons, 1958.

4. Frocht, M. M and Cheng, Y. F., "An Experimental Study of the Laws of Double Refraction in the Plastic State in Cellulose Nitrate - Foundations For Three-Dimensional Photoplasticity," Proceedings of the International Symposium on Photoelasticity, IIT, Chicago, 1961, pp. 195-216.

5. Ito, K., "New Model Materials for Photoelasticity and Photoplasticity," Experimental Mechanics, 2(12), December 1962, pp. 373-376.

6. Gurtman, G. A., Jenkins, W. C., and Tung, T. K., "Characterization of a Birefringent Material for Use in Photoelastoplasticity," Douglas Report SM 7796, January 1965.

7. Ramberg, W. and Osgood, W. R., "Description of Stress-Strain Curves of Three Parameters," NACA TN 902, 1943.

8. Mesnager, M., "Sur la Determination Optique des Tensions Interieures dan les Solides a Trois Dimensions," Compt. Rend. l'Acad. Sci., Vol. 190, 1930, pp. 1249-1250.

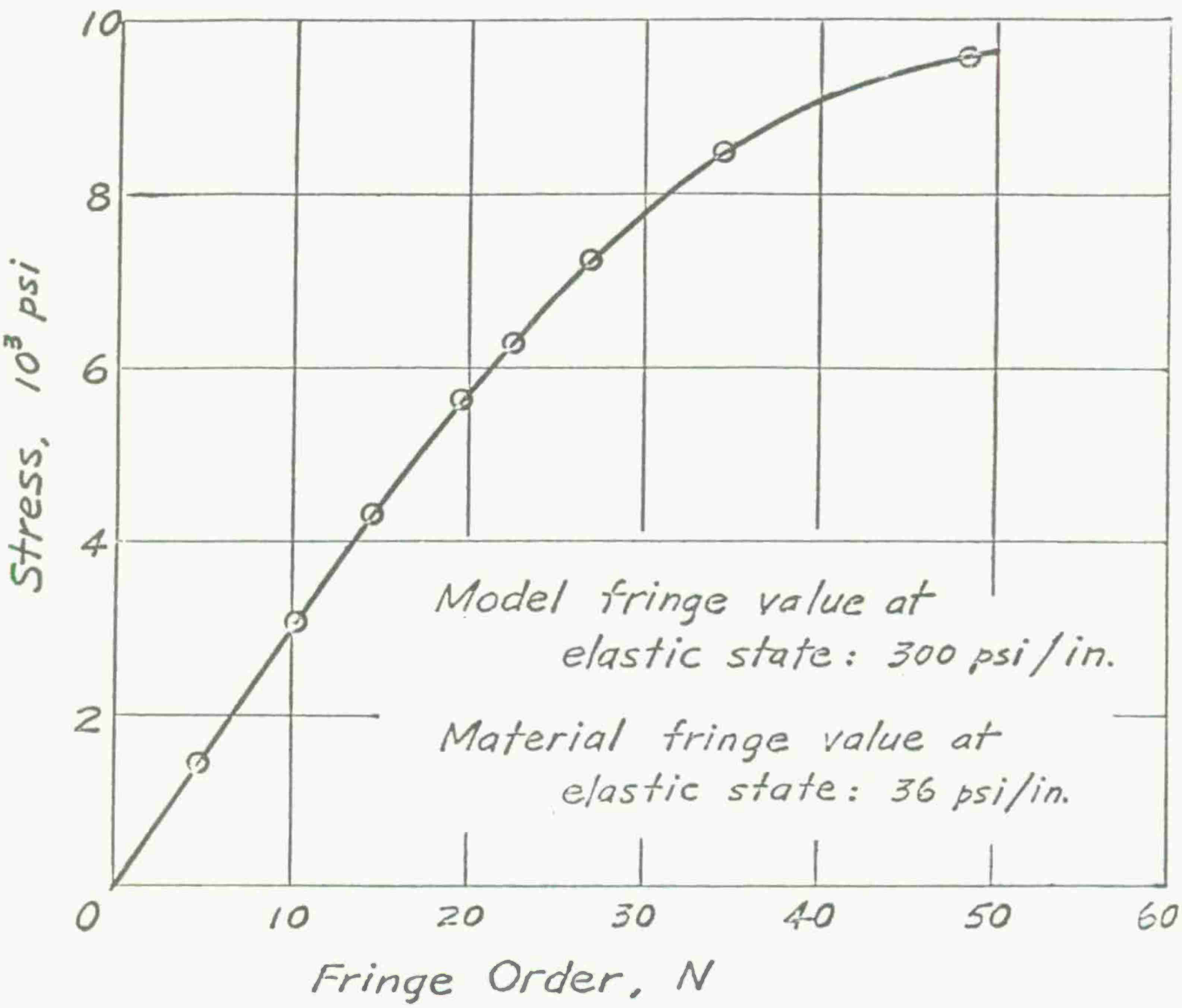

Figure 1. Stress-Fringe Curve for Polycarbonate.

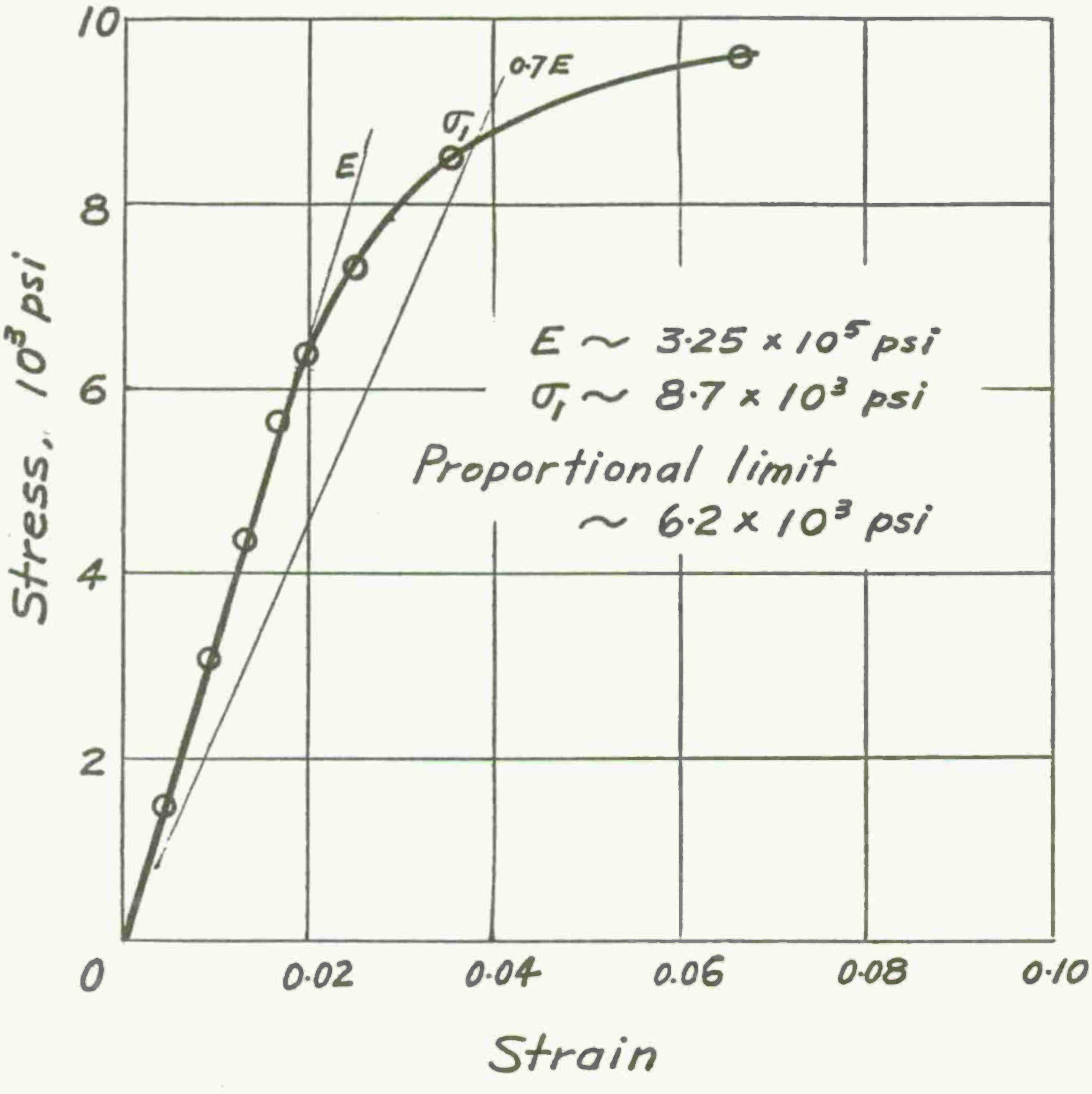

Figure 2. Stress-Strain Curve for Polycarbonate.

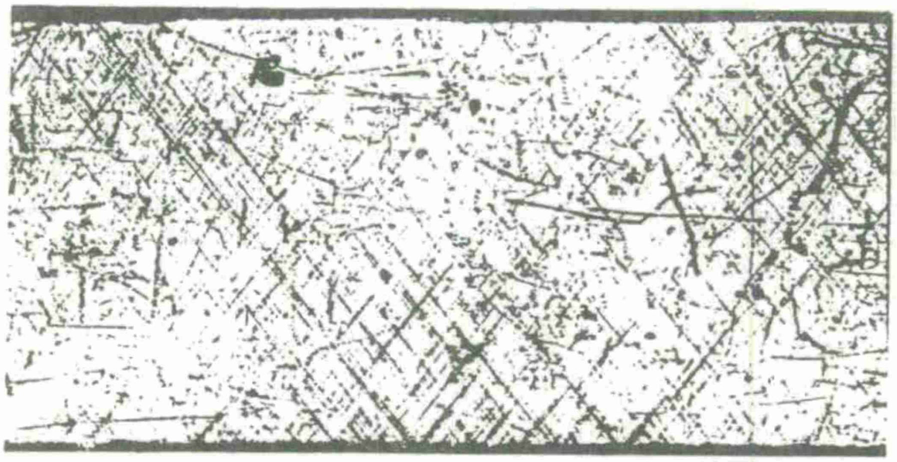

Figure 3. Photograph of Luder's Lines in Polycarbonate.

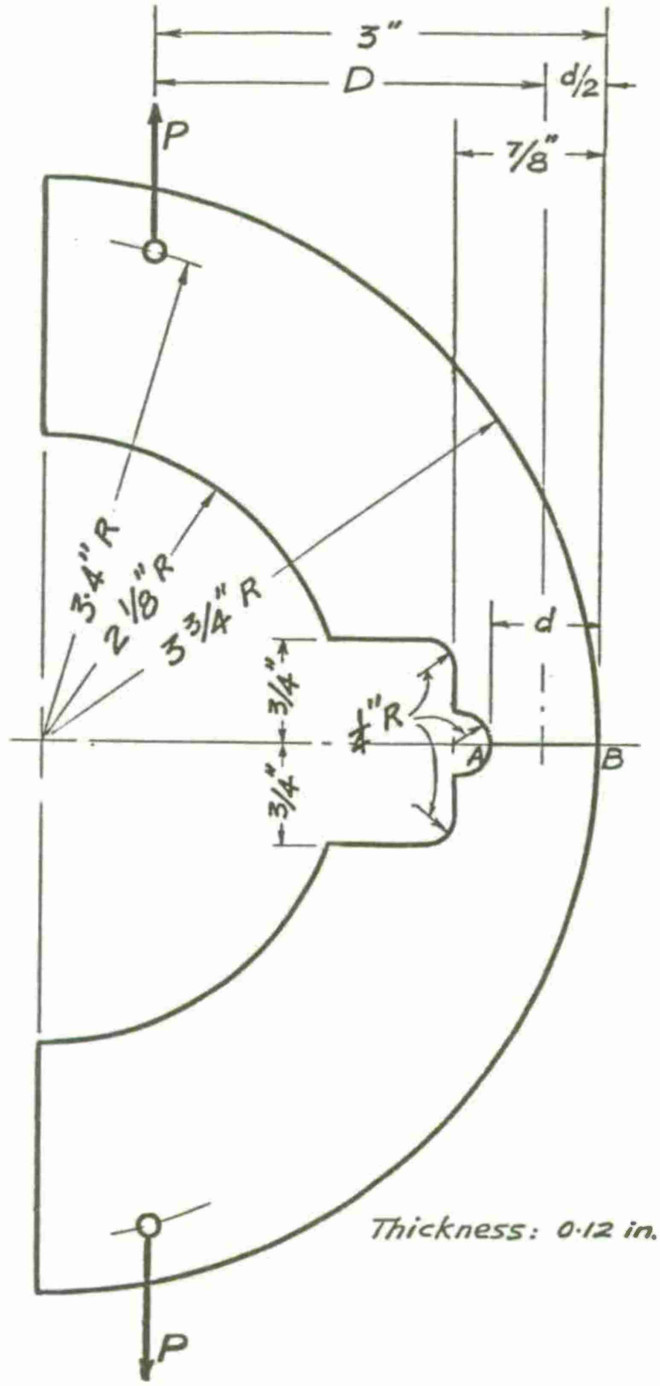

Figure 4. Sketch of C-Shaped Specimen.

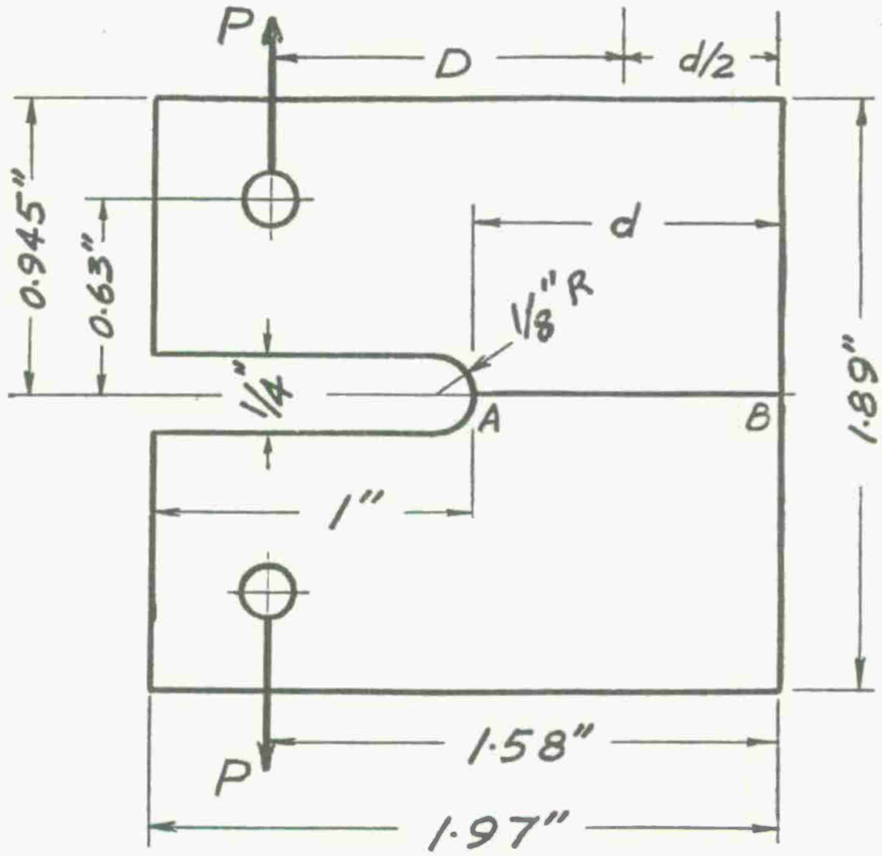

Thickness: 0.12 in.

Figure 5. Sketch of Compact Tensile Specimen.

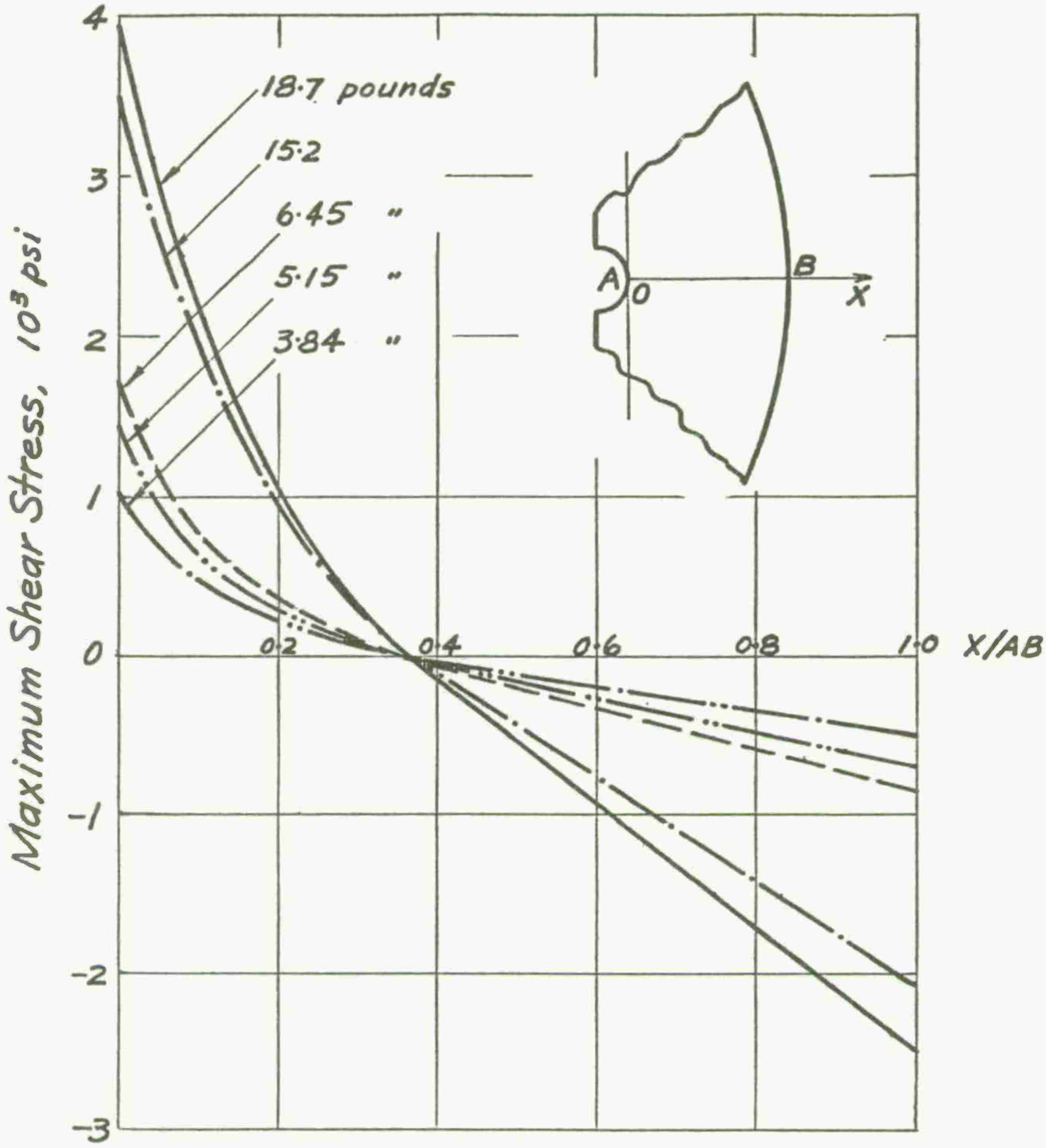

Figure 6. Maximum Shear Distribution Along Section AB in C-Shaped Specimen.

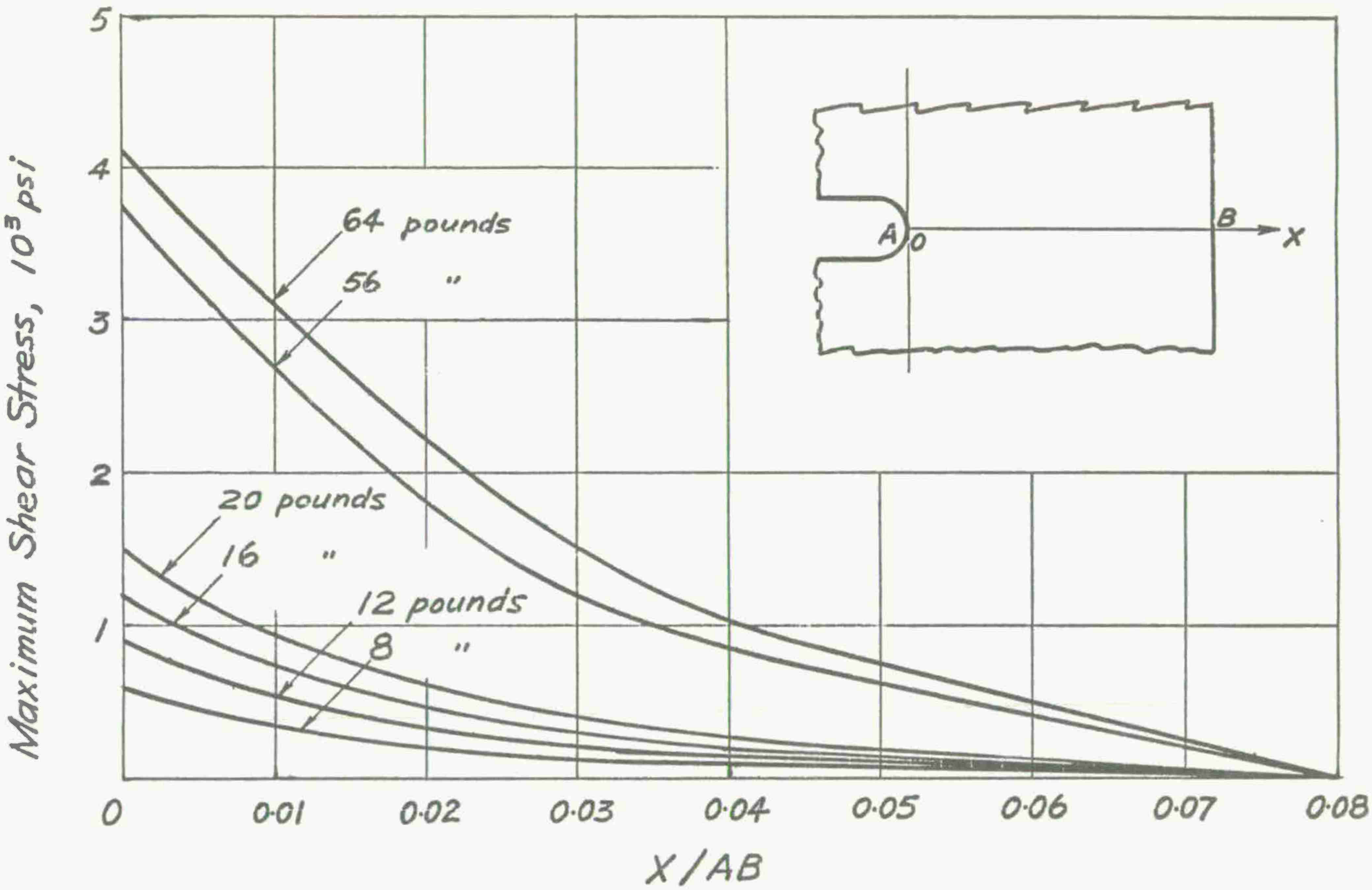

Figure 7. Maximum Shear Distribution Along Part of Section AB in Compact Tensile Specimen.

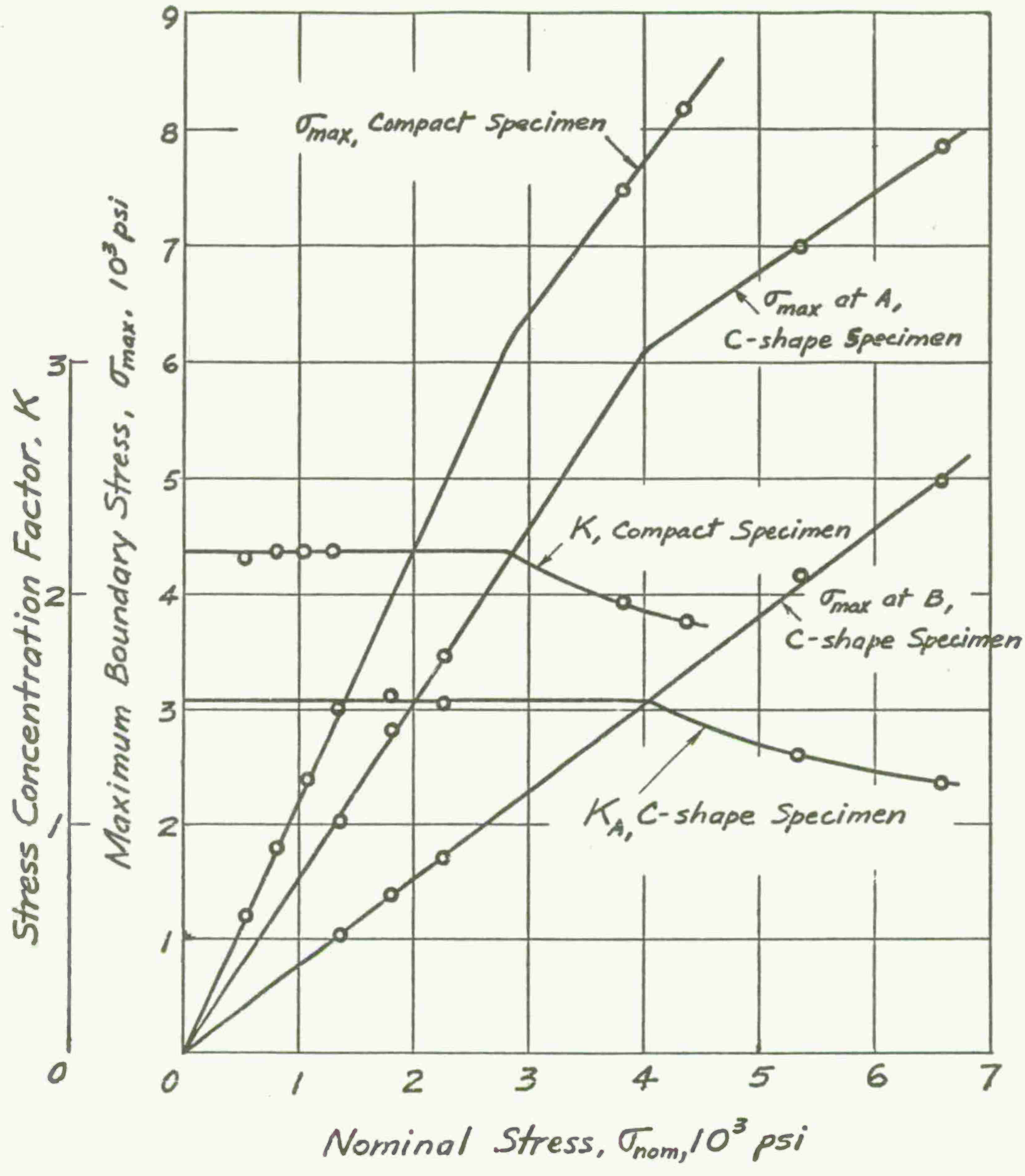

Figure 8. Curves of Stress Concentration Factor and Maximum Boundary Stress Versus Nominal Stress in C-Shaped and Compact Tensile Specimens.

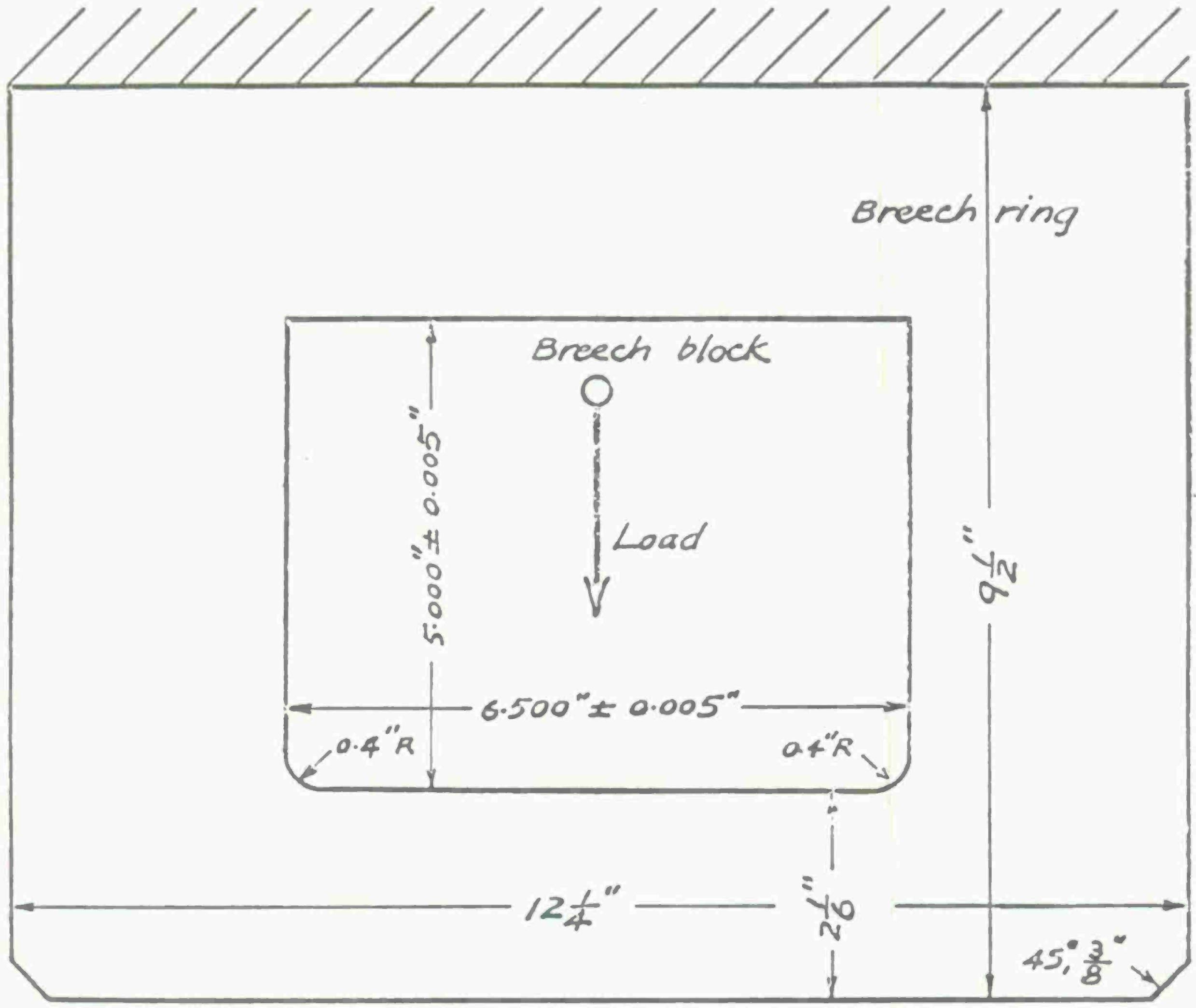

Figure 9. Sketch of a Breech Ring Section.

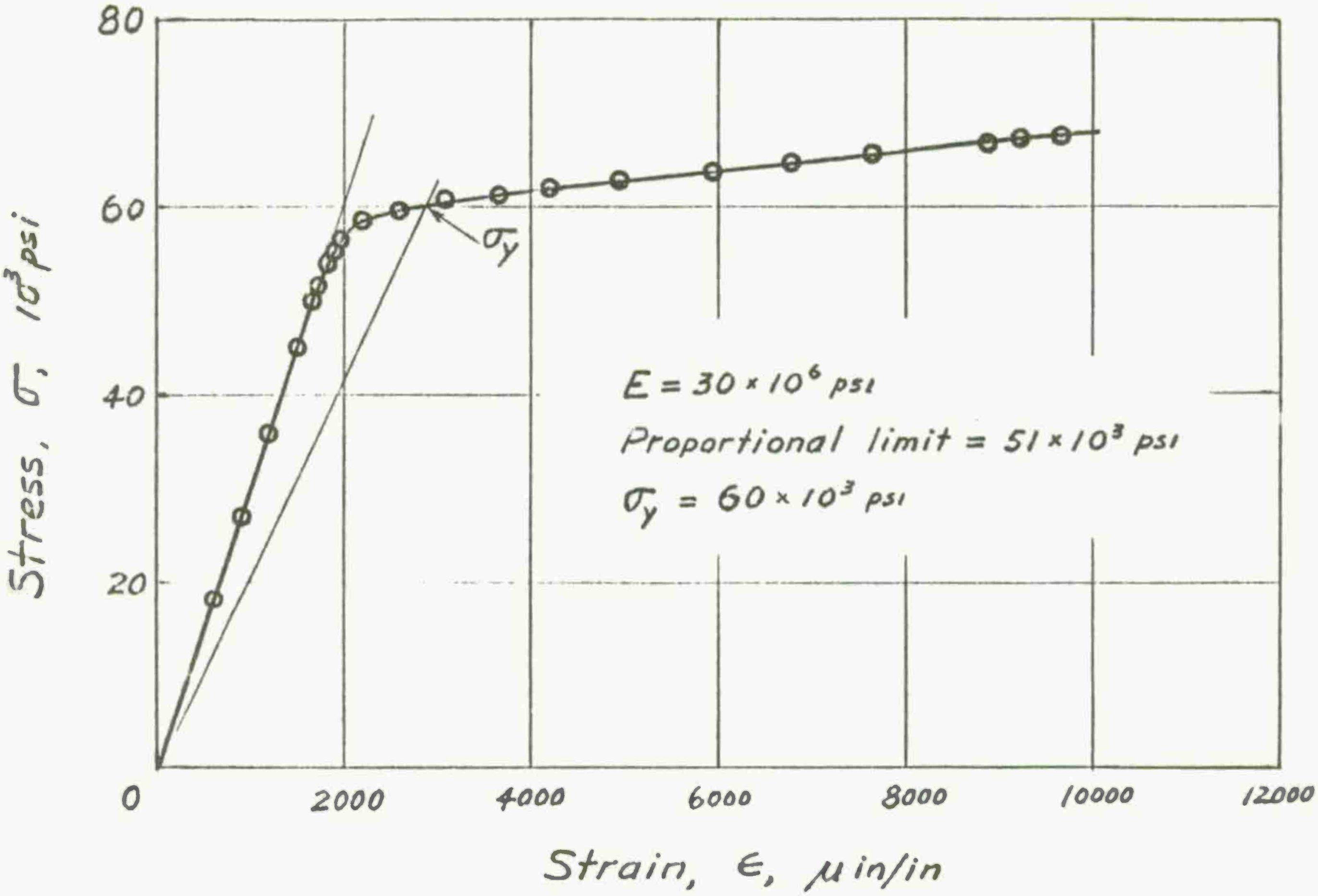

Figure 10. Stress-Strain Curve for Steel.

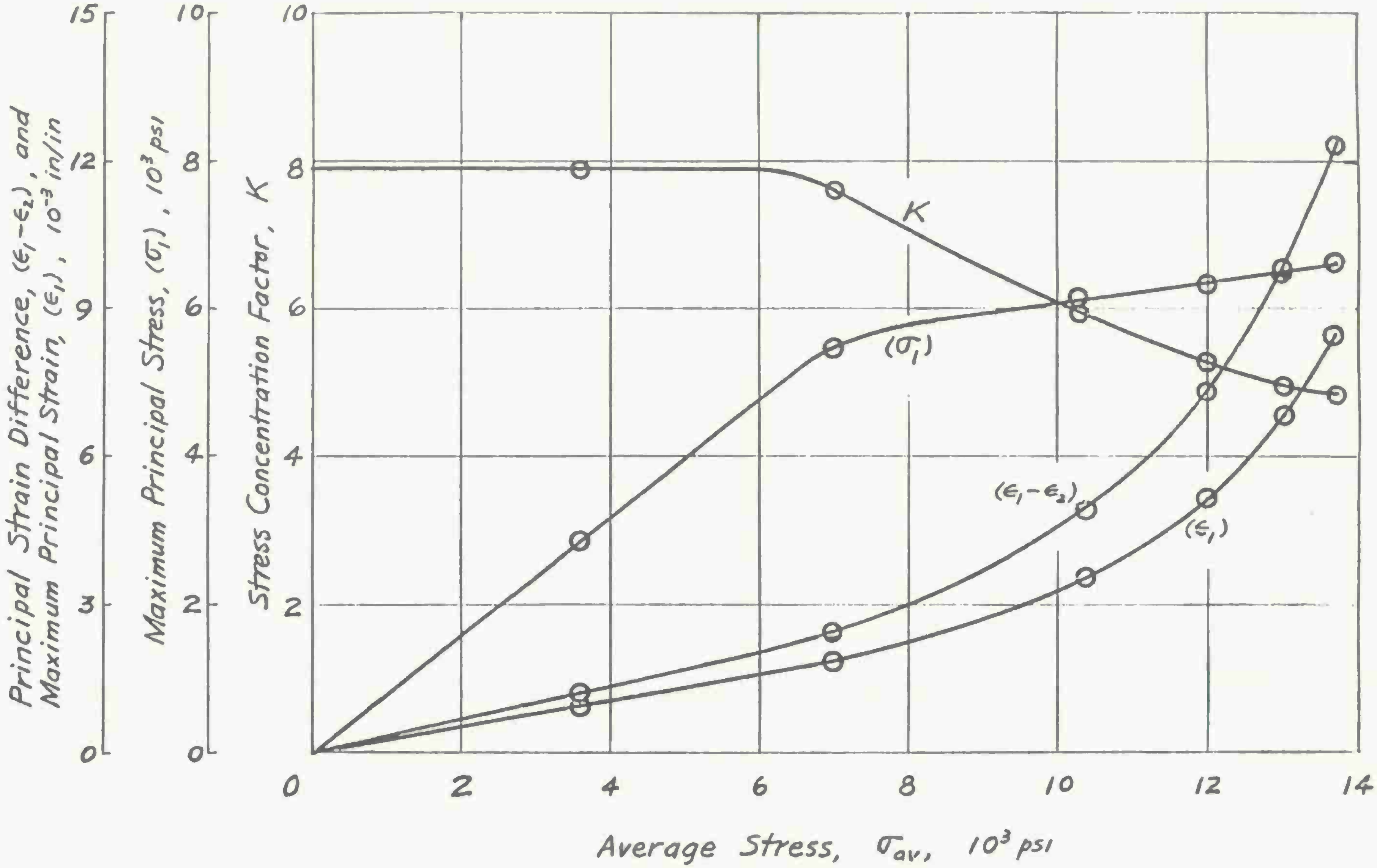

Figure 11. Curves of Principal Strain Difference, Maximum Principal Strain, Maximum Principal Stress, and Stress Concentration Factor Versus Average Stress at Lower Fillet of a Steel Breech Ring Section.

TECHNICAL REPORT INTERNAL DISTRIBUTION LIST

	NO. OF COPIES
CHIEF, DEVELOPMENT ENGINEERING BRANCH	
ATTN: SMCAR-LCB-D	1
-DA	1
-DP	1
-DR	1
-DS (SYSTEMS)	1
-DS (ICAS GROUP)	1
-DC	1
CHIEF, ENGINEERING SUPPORT BRANCH	
ATTN: SMCAR-LCB-S	1
-SE	1
CHIEF, RESEARCH BRANCH	
ATTN: SMCAR-LCB-R	2
-R (ELLEN FOGARTY)	1
-RA	1
-RM	2
-RP	1
-RT	1
TECHNICAL LIBRARY	5
ATTN: SMCAR-LCB-TL	
TECHNICAL PUBLICATIONS & EDITING UNIT	2
ATTN: SMCAR-LCB-TL	
DIRECTOR, OPERATIONS DIRECTORATE	1
DIRECTOR, PROCUREMENT DIRECTORATE	1
DIRECTOR, PRODUCT ASSURANCE DIRECTORATE	1

NOTE: PLEASE NOTIFY DIRECTOR, BENET WEAPONS LABORATORY, ATTN: SMCAR-LCB-TL, OF ANY ADDRESS CHANGES.

TECHNICAL REPORT EXTERNAL DISTRIBUTION LIST

	NO. OF COPIES
ASST SEC OF THE ARMY RESEARCH & DEVELOPMENT ATTN: DEP FOR SCI & TECH THE PENTAGON WASHINGTON, D.C. 20315	1
COMMANDER DEFENSE TECHNICAL INFO CENTER ATTN: DTIC-DDA CAMERON STATION ALEXANDRIA, VA 22314	12
COMMANDER US ARMY MAT DEV & READ COMD ATTN: DRCDE-SG 5001 EISENHOWER AVE ALEXANDRIA, VA 22333	1
COMMANDER ARMAMENT RES & DEV CTR US ARMY AMCCOM ATTN: SMCAR-LC	1
SMCAR-LCE	1
SMCAR-LCM (BLDG 321)	1
SMCAR-LCS	1
SMCAR-LCU	1
SMCAR-LCW	1
SMCAR-SCM-O (PLASTICS TECH EVAL CTR, BLDG. 351N)	1
SMCAR-TSS (STINFO) DOVER, NJ 07801	2
DIRECTOR BALLISTICS RESEARCH LABORATORY ATTN: AMXBR-TSB-S (STINFO) ABERDEEN PROVING GROUND, MD 21005	1
MATERIEL SYSTEMS ANALYSIS ACTV ATTN: DRXSY-MP ABERDEEN PROVING GROUND, MD 21005	1
COMMANDER US ARMY AMCCOM ATTN: SMCAR-ESP-L ROCK ISLAND, IL 61299	1
COMMANDER ROCK ISLAND ARSENAL ATTN: SMCRI-ENM (MAT SCI DIV) ROCK ISLAND, IL 61299	1
DIRECTOR US ARMY INDUSTRIAL BASE ENG ACTV ATTN: DRXIB-M ROCK ISLAND, IL 61299	1
COMMANDER US ARMY TANK-AUTMV R&D COMD ATTN: TECH LIB - DRSTA-TSL WARREN, MI 48090	1
COMMANDER US ARMY TANK-AUTMV COMD ATTN: DRSTA-RC WARREN, MI 48090	1
COMMANDER US MILITARY ACADEMY ATTN: CHMN, MECH ENGR DEPT WEST POINT, NY 10996	1
US ARMY MISSILE COMD REDSTONE SCIENTIFIC INFO CTR ATTN: DOCUMENTS SECT, BLDG. 4484 REDSTONE ARSENAL, AL 35898	2
COMMANDER US ARMY FGN SCIENCE & TECH CTR ATTN: DRXST-SD 220 7TH STREET, N.E. CHARLOTTESVILLE, VA 22901	1

NOTE: PLEASE NOTIFY COMMANDER, ARMAMENT RESEARCH AND DEVELOPMENT CENTER, US ARMY AMCCOM, ATTN: BENET WEAPONS LABORATORY, SMCAR-LCB-TL, WATERVLIET, NY 12189, OF ANY ADDRESS CHANGES.

TECHNICAL REPORT EXTERNAL DISTRIBUTION LIST (CONT'D)

	NO. OF COPIES
COMMANDER US ARMY MATERIALS & MECHANICS RESEARCH CENTER ATTN: TECH LIB - DRXMR-PL WATERTOWN, MA 01272	2
COMMANDER US ARMY RESEARCH OFFICE ATTN: CHIEF, IPO P.O. BOX 12211 RESEARCH TRIANGLE PARK, NC 27709	1
COMMANDER US ARMY HARRY DIAMOND LAB ATTN: TECH LIB 2800 POWDER MILL ROAD ADELPHIA, MD 20783	1
COMMANDER NAVAL SURFACE WEAPONS CTR ATTN: TECHNICAL LIBRARY CODE X212 DAHLGREN, VA 22448	1

	NO. OF COPIES
DIRECTOR US NAVAL RESEARCH LAB ATTN: DIR, MECH DIV CODE 26-27, (DOC LIB) WASHINGTON, D.C. 20375	1 1
COMMANDER AIR FORCE ARMAMENT LABORATORY ATTN: AFATL/DLJ AFATL/DLJG EGLIN AFB, FL 32542	1 1
METALS & CERAMICS INFO CTR BATTELLE COLUMBUS LAB 505 KING AVENUE COLUMBUS, OH 43201	1

NOTE: PLEASE NOTIFY COMMANDER, ARMAMENT RESEARCH AND DEVELOPMENT CENTER, US ARMY AMCCOM, ATTN: BENET WEAPONS LABORATORY, SMCAR-LCB-TL, WATERVLIET, NY 12189, OF ANY ADDRESS CHANGES.

U.S. OFFICIAL MAIL
WATERVLIET N.Y. MAY 2 '85
PENALTY FOR PRIVATE USE $300
U.S. POSTAGE 0.69
P.B. METER 6250010

BOOK RATE

DEPARTMENT OF THE ARMY
ARMAMENT RESEARCH AND DEVELOPMENT CENTER
BENÉT WEAPONS LABORATORY, LCWSL
US ARMY ARMAMENT, MUNITIONS AND CHEMICAL COMMAND
WATERVLIET, N.Y. 12189

OFFICIAL BUSINESS

SMCAR-LCB-TL

POSTAGE AND FEES PAID
DEPARTMENT OF THE ARMY
DOD - 314

OFFICIAL BUSINESS
PENALTY FOR PRIVATE USE, $ 300

COMMANDER
US ARMY AMCCOM
ATTN SMCAR-ESP-L
ROCK ISLAND, IL 61299

DA LABEL 18-1, 1 OCT. 74

RDD ______________
(AR 340-3)